Characterization of Extragalactic 24micron Sources in the Spitzer First Look Survey

Lin Yan[1], George Helou[1], D. Fadda[1], F.R. Marleau[1], M. Lacy[1], G. Wilson[1], B.T. Soifer[1,2], I. Drozdovsky[1], F. Masci[1], L. Armus[1], H.I. Teplitz[1], D.T. Frayer[1], J. Surace[1], L.J. Storrie-Lombardi[1], P.N. Appleton[1], S. Chapman[2], P. Choi[1], F. Fan[1], I. Heinrichsen[1], M. Im[4], M. Schmitz[3], D.L. Shupe[1], G.K. Squires[1]

ABSTRACT

In this Letter, we present the initial characterization of extragalactic $24\mu m$ sources in the Spitzer First Look Survey (FLS) by examining their counterparts at $8\mu m$ and R-band. The color-color diagram of 24-to-8 vs. 24-to-$0.7\mu m$ is populated with $18,734$ sources brighter than the 3σ flux limit of 110μJy. The data covers a total area of 3.7 sq.degrees. The 24-to-$0.7\mu m$ colors of these sources span almost 4 orders of magnitudes, while the 24-to-$8\mu m$ colors distribute at least over 2 orders of magnitudes. In addition to identifying $\sim 30\%$ of the total sample with infrared quiescent, mostly low redshift galaxies, we also found that: (1) 23% of the $24\mu m$ sources ($\sim$1200 per sq.degrees) with $\log_{10}(\nu f_\nu(24\mu m)/\nu f_\nu(8\mu m)) \geq 0.3$ and $\log_{10}(\nu f_\nu(24\mu m)/\nu f_\nu(0.7\mu m)) \geq 1.0$ are probably infrared luminous starburst galaxies with $L_{IR} \geq 3 \times 10^{11} L_\odot$ at $z \geq 1$. In particular, 13% of the sample (660 per sq.degrees) are $24\mu m$ detected only, with no detectable emission in either $8\mu m$ or R-band. With such extremely red IR/visible and mid-IR colors, these sources are the candidates for being ULIGs at $z \geq 2$. (2) 2% of the sample (85 per sq.degrees) have extremely red mid-infrared to optical color ($\log_{10}(\nu f_\nu(24\mu m)/\nu f_\nu(0.7\mu m)) \geq 1.5$) and fairly moderate 24-to-$8\mu m$ color ($\log_{10}(\nu f_\nu(24\mu m)/\nu f_\nu(8\mu m)) \sim 0.5$), and they are likely candidates for being dust reddened AGNs, like Mrk231 at $z \sim 0.6 - 3$. (3) We anticipate that some of these sources with extremely red colors may be new types of sources, since they can not be modelled with any familiar type of spectral energy distribution. We

[1]Spitzer Space Telescope Science Center, California Institute of Technology, 1200 East California Boulevard, MS 220-6, Pasadena, CA 91125; Send offprint requests to Lin Yan: lyan@ipac.caltech.edu.

[2]The Caltech Optical Observatories, Caltech, Pasadena, CA 91125

[3]IPAC, Caltech, Pasadena, CA 91125

[4]School of Earth and Environmental Sciences, Seoul National University, Shillim-dong, Kwanak-gu,Seoul, S. Korea

find that close to 38% of the $24\mu m$ sources have optical R fainter than 23.0 vega magnitude, and 17% of these have no detectable optical counterparts brighter than R limit of 25.5mag. Optical spectroscopy of these optical extremely faint $24\mu m$ sources would be very difficult, and mid-infrared spectroscopy from the Spitzer would be critical for understanding their physical nature.

Subject headings: galaxies: infrared galaxies – galaxies: starbursts – galaxies: surveys – galaxies: high-redshifts – galaxies: AGNs

1. Introduction

The far-IR background detected by *COBE* (Puget et al. 1996; Fixsen et al. 1998) peaks around $\sim 200\mu m$ with energy comparable to the optical/UV background. This implies that 50% of the integrated rest-frame optical/UV emission is thermally reprocessed by dust and radiated at mid to far-infrared. Thus, dust enshrouded galaxies with high IR/visible ratios, particularly Ultraluminous Infrared Galaxies (ULIRGs, $L_{fir} > 10^{12}$ L$_{\odot}$, $L_{fir}/L_{vis} >$a few), make a significant contribution to the total energy budget and star formation over the history of the Universe. Deep surveys based on the rest-frame UV/optical do not provide a complete census of galaxy populations, and their measurements of luminosity and SFR are only lower limits (Meurer, Heckman & Calzetti 1999; Yan et al. 1999). Deep ISO and sub-mm SCUBA observations have shown that the integrated luminosity density from dusty sources peak around $z \sim 1$, roughly a factor of 4 - 5 higher than those measured from the rest-frame optical surveys (Serjeant et al. 2000; Elbaz et al. 1999; Gruppioni et al. 2003; Blain et al. 1999). This peak in the SFR appears to be relatively flat out to $z \sim 2 - 4$ (Franceschini et al. 2001; Franceschini et al. 2002; Elbaz et al. 2002; Lagache et al. 2003).

While ISO deep surveys probe primarily galaxies at $z < 1$ (Genzel & Cesarsky 2000), and sub-mm SCUBA observations are limited to a small number of high luminosity dusty sources at $z > 2$ (Chapman et al. 2003), the dusty universe at $z > 1$ is largely unexplored by systematic surveys in the mid-to-far infrared wavelength. The $24\mu m$ imaging camera on the Spitzer Space Telescope (Werner et al. 2004) provides us the first opportunity to do this. IRAS and ISO studies have shown that mid-infrared emission is a good indicator of the bolometric IR luminosity (Soifer et al. 1987; Surace et al. 1998; Elbaz et al. 2002; Chary & Elbaz 2001). At $0.7 < z < 2.5$, the $24\mu m$ band samples redshifted, rest-frame 6–$12\mu m$ emission from polycyclic aromatic hydrocarbons (PAH) and very small dust grains in dusty galaxies, making it the most sensitive window to probe the high-redshift infrared bright galaxies.

In this Letter, we make the first attempt to characterize the properties of $24\mu m$ selected galaxies within the Spitzer First Look Survey (FLS)[1]. This paper studies the distribution in the 24-to-8 and 24-to-0.7micron (R(24,8) and R(24,0.7)[2] color-color diagram of 18,734 $24\mu m$ selected sources over an area of 3.7 square degree. The R(24,8) and R(24,0.7) colors are indicative of the intrinsic slopes of the spectral energy distribution (SED) as well as dust extinction and K corrections. This Letter pays special attention to the populations with extremely red 24-to-8 and 24-to-0.7μm colors, and estimate their surface densities. Throughout this paper, we adopt $H_0 = 70$km/s/Mpc, $\Omega_M = 0.3$ and $\Omega_\Lambda = 0.7$. The magnitude system is in vega.

2. Observations and Data Reduction

2.1. Image Reduction and Source Extraction

Table 1 summarizes all of the data went into the analyses in this Letter. Specifically, the $24\mu m$ flux cutoff of 110μJy is for SNR of 3σ, which is computed at the peak pixel. This is a conservative measurement in comparison with the SNR calculated through a large aperture. After the reliable sources were selected with this conservative flux limit, we can use lower SNR (2σ) to estimate the flux limits for sources not detected in the $8\mu m$ and R band. The Spitzer data were taken with the IRAC and MIPS cameras (Fazio et al. 2004; Rieke et al. 2004). The $8\mu m$ and $24\mu m$ data cover an area of 3.7 square degrees, where these two datasets overlap. Both IRAC and MIPS raw data were processed and mosaiced together by the pipeline provided by the Spitzer Science Center (SSC). Additional corrections to the Basic Calibrated Data (BCD) images were included, see Lacy et al. (2004) and Fadda et al. (2004) for details. The $8\mu m$ source catalog is generated using SExtractor (Bertin & Arnout 1996). We used the photometry within a $6.1''$ diameter aperture. The total fluxes are obtained by applying the appropriate aperture corrections, which are scaled to the $24''$ diameter aperture. This is at most around 30% (Lacy et al. 2004). The $24\mu m$ source catalog was generated using StarFinder (Diolaiti et al. 2000). The aperture correction for obtaining the total $24\mu m$ flux is $\sim$10% (Fadda et al. 2004a). The R-band images were taken with the MOSAIC-1 camera on the 4 m telescope at the Kitt Peak National Observatory. The reduced and stacked images as well as source catalogs have been publicly released, and the detailed description of the observations, data reduction and catalogs can be found in Fadda et al. (2004b).

---

[1]see http:// ssc.spitzer.caltech.edu/fls for details

[2]here we define R(24,8) $\equiv \log_{10}(\nu f_\nu(24\mu m)/\nu f_\nu(8\mu m))$, and R(24,0.7) $\equiv \log_{10}(\nu f_\nu(24\mu m)/\nu f_\nu(0.7\mu m))$

2.2. Bandmerged Catalog

We cross-identified the $24\mu m$ sources in the $8\mu m$ and R-band by simple positional matching. The IRAC astrometry was fine-tuned using the reference positions from the 2MASS point sources. The MIPS $24\mu m$ images were aligned with the VLA 20cm radio positions. The mean positional differences between R and $24\mu m$ for bright and unsaturated sources are $0.1''$ with a rms of $0.4''$ in both right ascension and declination. Similarly, we found the $< \Delta RA >= 0.04'' \pm 0.6''$ and $< \Delta DEC >= 0.03'' \pm 0.6''$ between the IRAC $8\mu m$ and R-band images. We use $2''$ matching radii, generously chosen to allow somewhat larger astrometric uncertainties for fainter sources. Multiple matches between the 24 and $8 \mu m$ catalogs are neglible, less than 0.05%. The fraction of multiple matches between the 24 micron and R-band catalogs is higher, about 7%. In these cases, we choose the closest matches in the positional centroids between the two bands. Stellar contamination for a $24\mu m$ selected sample is expected to be low since we are sampling the tail of the Rayleigh-Jeans energy distribution and the FLS galactic latitute is $37°$. Stars brighter than R of 20 mag can be easily identified on the R-band images. For sources with $20 < R < 23$, we used the stellarity index (> 0.8 sources are stars) measured with SExtractor. The total stellar contamination is estimated to be only 7.5%. We have visually spot-checked the final catalog on the image display.

3. Results

We have a total of 18,734 sources, which are detected at $24\mu m$ with fluxes brighter than 3σ 110μJy. Of these, close to half of them have good detections in all three bands. The remaining half of the $24\mu m$ sources have no detections in one or both of the $8\mu m$ and R bands. Plate 1 gives the 2-dimensional stamp images of a set of representative examples. As shown, some bright $24\mu m$ sources have no counterparts at either $8\mu m$ or R band. These cases will be discussed in detail below.

The main result of this Letter is presented in Figure 2a, showing the 24-to-8 and 24-to-$0.7\mu m$ color-color distribution of our sources. Figure 2b presents the expected color-color tracks as a function of redshifts computed from known types of SED templates. Figure 2a shows a broad correlation between higher IR/visible ratios and IR colors, indicative of more intensely heated dust, similar to the trends seen in the IRAS data (Soifer & Neugebauer 1991). Using this figure, we can crudely classify various types of $24\mu m$ selected sources by comparison with the expected colors of known SED templates as well as with known objects in the FLS region. The SED templates include Arp220 and M82 (Silva et al. 1989; Chary & Elbaz 2001), NGC253 (Fadda et al. 2002), radio-quiet QSO, M51 & NGC1068 (Dale et
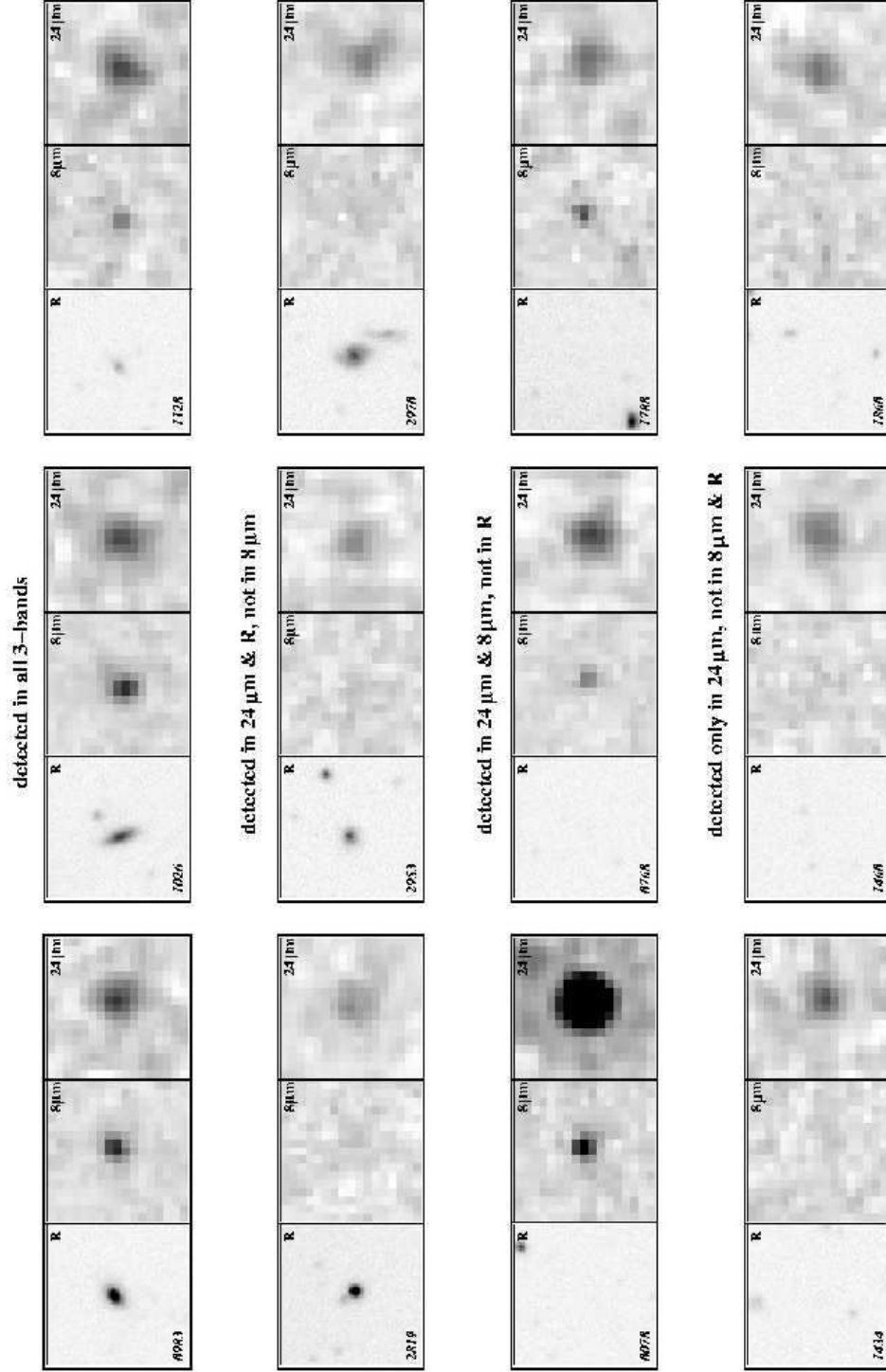
Fig. 1.— This figure is also included as fig1.jpg. **Plate 1** shows a few representative examples of four types of $24\mu m$ sources: sources detected in all three bands; sources detected in $8\mu m$ but not in R; sources detected in R but not in $8\mu m$; $24\mu m$ detected sources only.

al. 2001; Dale & Helou 2002). To show the colors of an early type galaxy, we construct the SED for the bulge of M31 within an aperture of $4'$ diameter using the near-IR and IRAS data published in Soifer et al. (1986). The optical part of the SED for M31 bulge was taken as a 10 Gyr old elliptical SED from Bruzual & Charlot[3], then scaled and matched with the infrared part to produce a full SED covering from 0.1 — 100 μm.

3.1.   Infrared Quiescent Sources

Comparing Figure 2a and 2b, the color-color distribution can be crudely classified into two extreme regions — the infrared quiescent region where $R(24, 8) \leq 0.5$ and $R(24, 0.7) \leq 0$, the infrared luminous region with $R(24, 8) > 0.5$ and $R(24, 0.7) > 1$. The region between these two probably contains a mixture of starbursts and normal galaxies at various redshifts. In Figure 2a, the black points occupy the most of the first region. These are $24\mu m$ sources which have significant detections at $8\mu m$ as well as R-band. Comparing with the model color-color tracks, we infer that the sources with $R(24, 8) \leq 0.5$ and $R(24, 0.7) \leq 0$ are primarily normal, infrared faint galaxies at low redshift ($z < 0.7$) and optically selected QSOs with a wider redshift distribution. Figure 3a,b show the differential number counts as functions of colors, $R(24, 8)$ and $R(24, 0.7)$. A little less than 30% of the total population are infrared quiescent spirals and early type galaxies at low redshifts as well as optically selected QSOs. The galaxies with extremely low 24-to-8micron flux ratio are old bulges, such as M31. Their colors can not be explained by pure interstellar dust emission, and they must have substantial stellar photospheric and dust envelope contributions coming into the $8\mu m$ band.

To test further this interpretation of Figure 2a, we have used the NED extragalactic database and identified the sources in our catalog with the low redshift galaxies (magenta triangles) and optically selected QSOs (cyan triangles) from the Sloan Digital Sky Survey[4]. The locations of these sources with known types and redshifts in Figure 2a generally confirm our interpretation. The cyan points in Figure 2a can be well explained by the computed colors of a radio-quiet QSO SED template in Figure 2b. These optically selected QSOs have fairly flat SEDs (Neugebauer et al. 1987; Sanders et al. 1989), therefore, their colors are around $R(24, 8) \sim 0$ and $R(24, 0.7) \sim 0$ with very little change with redshifts. One specific example is a sloan QSO at $z = 4.5445$, with the fluxes of 744μJy, 98 μJy and 27 μJy at the 24, 8 and 0.7μm respectively, thus $R(24, 8) = 0.4$ and $R(24, 0.7) = -0.1$.

---

[3]ftp://gemini.tuc.noao.edu/pub/charlot/bca5

[4]http://www.sdss.org

3.2. The Nature of the Extreme $24\mu m$ Populations

Figure 2a illustrates the colors of four types of sources marked with small black, red, green and blue points. The objects indicated with black points have been discussed before. The red points consist 31% of the $24\mu m$ sources, which are detected only in R-band, but not at the $8\mu m$-band. The green points represent 4%, with detections only in $8\mu m$, but no counterparts in R brighter than 2σ limit of 25.5mag. Finally, 13% of the sample (660 objects per sq.degree) are not detected in either $8\mu m$ or R, shown as small blue points in Figure 2a. The mean fluxes of the objects marked as red, green and blue points are roughly between 230-360μJy. One of the most interesting sources revealed by the $24\mu m$ images are ones which have $R(24, 0.7) > 1$ and $R(24, 8) > 0.3$ in Figure 2a. These sources are candidates for being luminous starburst galaxies at $z \geq 1$. Using this color-color cut, we estimate that 23% ($\sim$1200 per sq.degree) of our $24\mu m$ sample are such objects. In particular, those sources detected only at $24\mu m$ (blue points) are likely to be ULIGs at $z > 2$ (660 per sq.degrees). At $z = 1$, our 3σ $24\mu m$ flux limit of 110μJy corresponds to the observed luminosity νL_ν of $2 \times 10^{10}L_\odot$. If we ignore the filter difference between the Spitzer $24\mu m$ and the IRAS $12\mu m$ (the $24\mu m$ bandwidth is about half of the $12\mu m$ filter), the $z = 1$ observed $24\mu m$ luminosity is roughly the rest-frame IRAS $12\mu m$ luminosity. The total infrared luminosity $L_{IR}(8 - 1000\mu)$ is correlated with IRAS $12\mu m$ luminosity $\nu L_\nu(12\mu)$, in the form of $L_{IR} = 0.89 \times \nu L_\nu(12\mu)^{1.094}L_\odot$, as derived from the IRAS Revised Bright Galaxy Sample (Soifer et al. 1987; Chary & Elbaz 2001). This implies that the $z > 1$ starbursts should have $L_{IR} \geq 2.7 \times 10^{11}L_\odot$. As suggested by the $24\mu m$ source counts (Marleau et al. 2004), the FLS data may reach $z \sim 2$ starburst population. Our flux limit implies that at $z \sim 2$, the infrared luminosity L_{IR} should be brighter than $2 \times 10^{12}L_\odot$.

Another interesting population are sources with $R(24, 0.7) > 1.5$ but with a fairly constant $R(24, 8) \sim 0.5$. Figure 2b suggests that these sources are likely to be dust heavily reddened AGNs like NGC 1068, or Mrk231 at $z > 1$. These sources could be separated from the general population using the IRAC 8-to-4.5 and 5.8-to-3.5micron color-color selection (Lacy et al. 2004). The surface density of these dusty AGNs are on the order of $\sim$85 per sq.degree, and they constitute $\sim$2% of the total $24\mu m$ population. To confirm our prediction that we can use $R(24, 8)$ vs. $R(24, 0.70$ to select high redshift, infrared luminous galaxies, we mark on Figure 2a the several $24\mu m$ sources detected with the SCUBA at $850\mu m$ (see Frayer et al. 2004 for detail). These SCUBA sources could be at $z \sim 1-3$, as shown in Chapman et al. (2003). Our computed color-color tracks in Figure 2 is to illustrate in a broad sense what range of colors each type of sources should have. A small number of sources with extremely red 24-to-8 and 24-to-R colors can not be all explained by models with known type of SEDs. This could be suggestive of potentially new classes of objects.

We examine the optical brightness of $24\mu m$ selected sources in Figure 4, showing the $R(24, 0.7)$ and $R(24, 8)$ as a function of R magnitude for the $24\mu m$ sources. Close to 36% of the $24\mu m$ sources have R magnitudes fainter than 23.0mag. Such a faint optical magnitude might suggest that they are at $z > 0.5$, supported by the measurements from optical R band selected redshift surveys (Lilly et al. 1996; Cohen et al. 2001). Many of these sources are well within the brightness regime of the 10 meter classes telescopes for obtaing the optical spectroscopic redshifts. However, the $24\mu m$ sources without R counterparts fainter than 2σ of 25.5mag will be difficult to follow-up with the optical spectroscopy. The redshifts and physical natures of these sources could be measured using the mid-infrared spectrograph (IRS) from the Spitzer InfraRed Spectrometer. Particularly, for sources with $24\mu m$ fluxes brighter than 750μJy, the IRS would be sensitive enough to obtain good SNR low resolution spectra covering $5\mu m$ to $38\mu m$ with a total of (1-2) hours of integration. We have a total of 46 sources which have $24\mu m$ fluxes brighter than 750μJy and R-band magnitude fainter than 25.0mag.
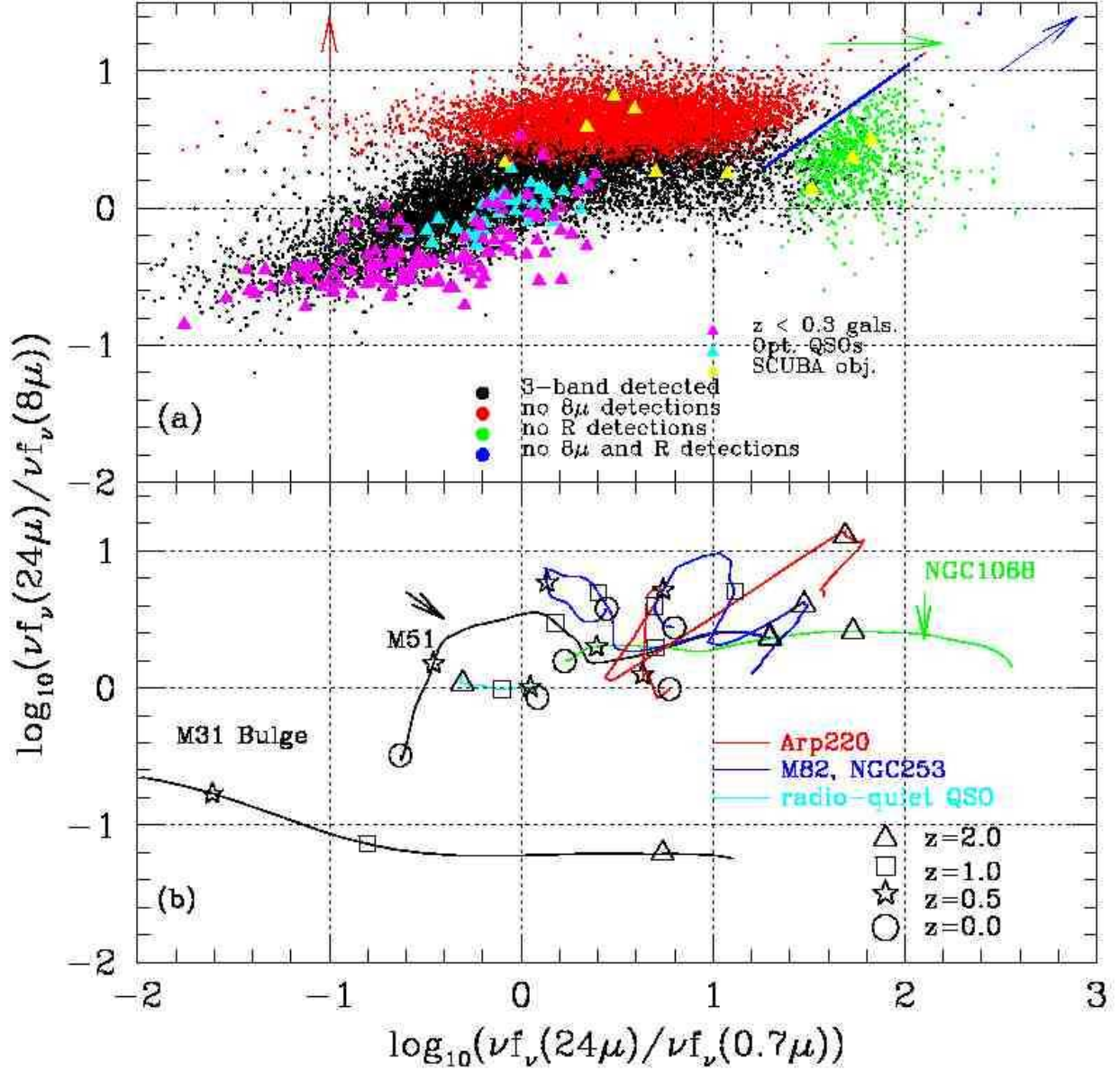
Fig. 2.— This figure is also included as fig2.jpg. The color-color plot between $\log_{10}(\nu f_\nu(24\mu)/\nu f_\nu(8\mu))$ and $\log_{10}(\nu f_\nu(24\mu)/\nu f_\nu(R))$. **Panel a** shows the data for a total of 18,734 sources selected at $24\mu m$ in the FLS main field. The small black points are sources detected in all three bands; the small green points are sources only detected in the $8\mu m$ bands, and not detected in the optical R-band; the small red points indicate sources with significant detections in the R-band, but no detections at $8\mu m$; the small blue points represents the sources detected only in the $24\mu m$. To illustrate the lower limits in colors, we marked the arrows with corresponding color code for the red, green and blue sources. The big yellow triangles are sources with SCUBA detections, the cyan triangles are optically selected QSOs with known redshifts and spectra; the magenta triangles are low redshift galaxies identified from the SDSS. **Panel b** shows the expected color tracks as a function of redshifts computed from a set of SED templates for local known galaxies.
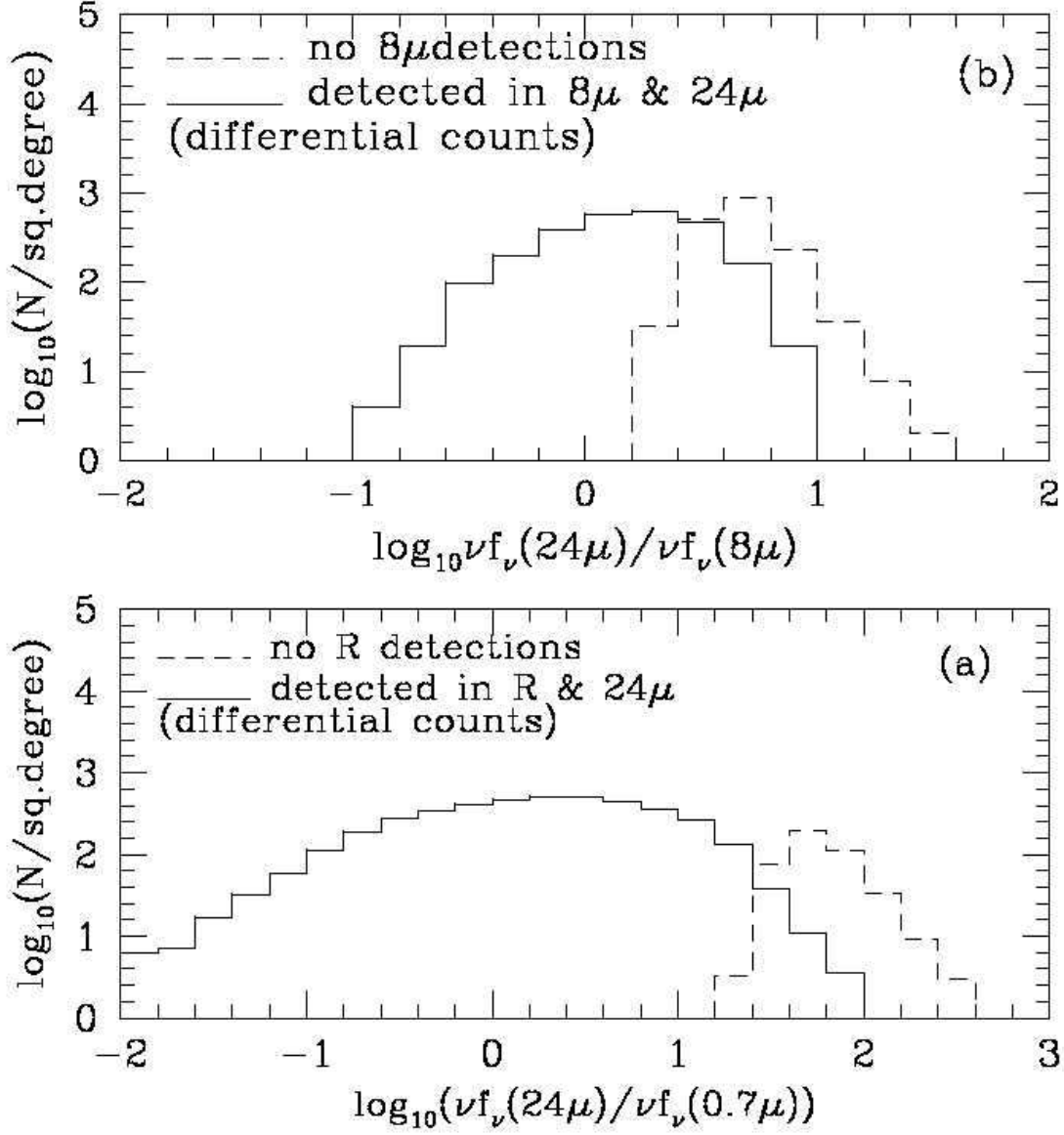
Fig. 3.— This figure is also included as fig3.jpg. The $24\mu m$ source counts as functions of $R(24, 0.7)$ and $R(24, 8)$ The dashed lines in both panels are sources with flux limits in either the $8\mu m$ or the R-band. The number counts are differential, and the y-axis has units of number of sources per square degree. The total area coverage is 3.7 sq.degree, and the total number of sources is 18,734.
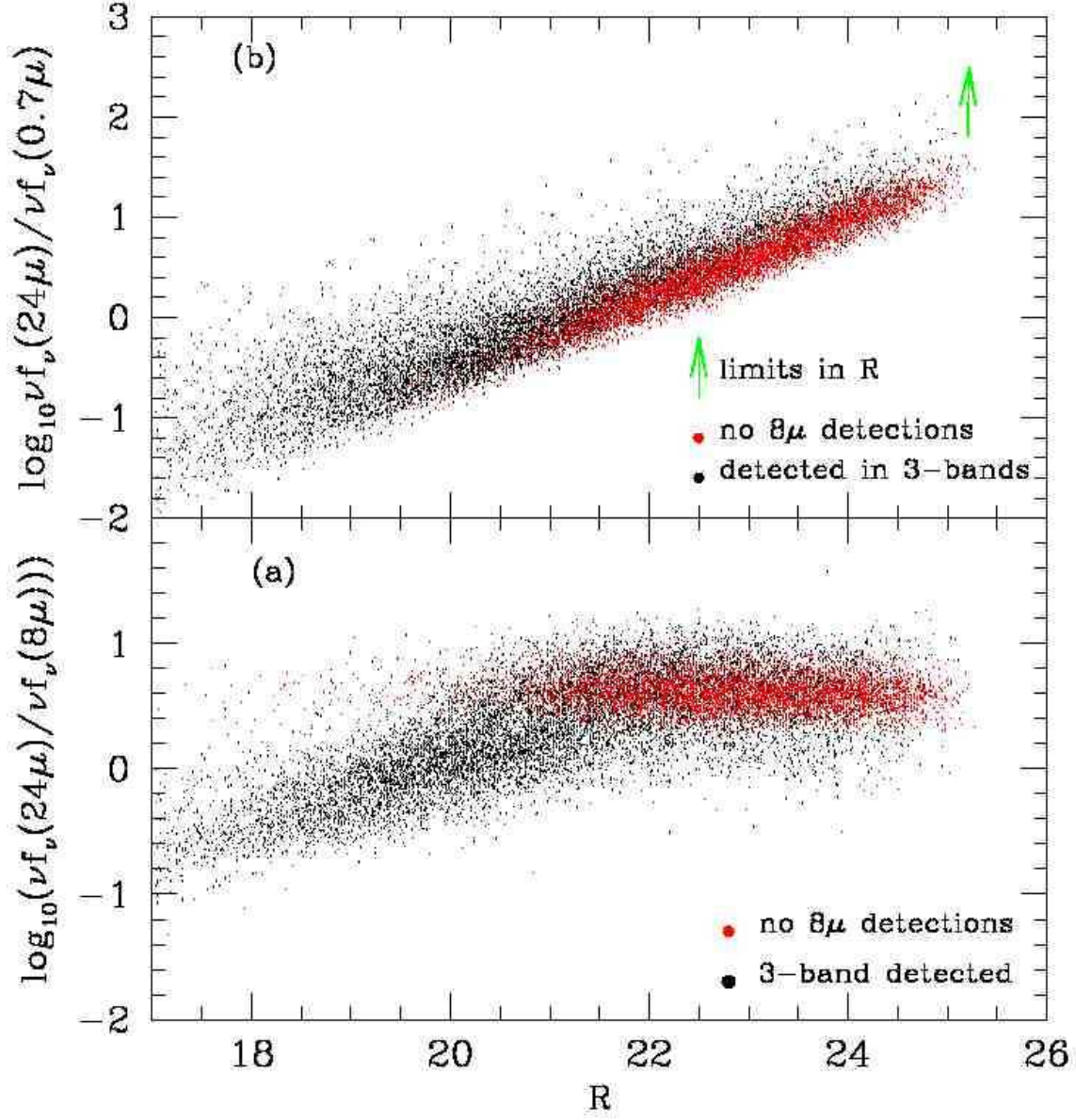
Fig. 4.— This figure is also included as fig4.jpg. **Panel a** shows the 24-to-8μm flux ratio versus R magnitude for the 24μm selected sample. **Panel b** shows the color-magnitude diagram of the 24-to-0.7μm flux ratios versus R magnitude.

Table 1.   Summary of Optical, IRAC $8\mu m$ and MIPS $24\mu m$ Observations

λ_{cent} (μm)	0.7	8.0	24.0
FWHM ($''$)	1.0	2.2	5.5
Flux Limits	25.5mag[a]	20μJy[a]	110μJy[a]
$\nu f_\nu(lim)$(ergs/s/cm^2)	1.3e-15[b]	3.75e-15	24e-15
<Exp. Time> (sec)	1800	60	80

[a]Here R of 25.5mag is a 2σ limit within a $3''$ diameter aperture. The $8\mu m$ flux 20μJy is a 2σ limit, included aperture correction. The $24\mu m$ flux 110μJy is a flux cutoff where the SNR at the peak pixel is greater than or equal to 3σ. See the text for details.

[b]$f_R(0mag)$ = 2780Jy (Neugebauer 1997, private communication)

REFERENCES

Blain et al. 1999, MNRAS, 302, 632.

Chapman, S. et al. 2003, Nature, 422, 695

Chary & Elbaz 2001, ApJ, 556, 562

Cohen, J. et al. 2001, AJ, 121, 2895

Dale, D. & Helou, G. 2002, ApJ, 576, 159

Dale, D. et al. 2001, ApJ, 549, 215

Diolaiti, E. et al. 2000, SPIE, 4007, 879

Elbaz, D. et al. 1999, A&A, 351, 37

Elbaz et al. 2002, A&A, 384, 848.

Fadda et al. 2002, A&A, 383, 838

Fadda, D., et al. 2004a, in this volume

Fadda, D., Jannuzi, B., Ford, A., & Storrie-Lombardi, L.J., 2004b, AJ, in press [astro-ph/0403490]

Fazio, G. et al. 2004, in this volume

Fixsen, D.J., et al. 1998, ApJ, 508, 123

Franceschini et al. 2001, A&A, 378, 1

Franceschini et al. 2002, ApJ, 568, 470.

Genzel & Cesarsky 2000, ARA&A, 38, 761.

Gruppioni, C. et al. 2003, MNRAS, 341, 1

Lacy, M. et al. 2004, ApJ, in this volume

Lagache et al. 2003, MNRAS, 338, 555.

Lilly, S. et al. 1996, ApJL, 460, 1

Meuer, Heckman & Calzetti 1999, ApJ, 521, 64.

Marleau, F. et al. 2004, in this volume

Neugebauer, G., Green, R.F. et al. 1987, ApJS, 63, 615

Puget et al. 1996, A&A, 308, L5.

Rieke, G., et al. 2004, in this volume

Serjeant et al. 2000, MNRAS, 317, 29.

Silva et al. 1998, ApJ, 509, 103.

Sanders, D.B., Phinney, E.S., Neugebauer, G., Soifer, B.T., Matthews, K., 1989, 347, 29

Soifer, B.T., Sanders, D.B., Madore, B.F. et al. 1987, ApJ, 320, 238.

Soifer, B.T., Rice, W.L., Mould, J.R., Gillett, F.C., Rowan-Robinson, M., habing, H.J, 1986, ApJ, 304, 651

Soifer, B.T., Neugebauer, G., 1991, AJ, 101, 354.

Surace, J., 1998, Ph.D thesis, University of Hawaii.

Werner, M. et al. 2004, in this volume

Yan et al. 1999, ApJ, 519, L47.